DOI:10.1021/jf100342u

JOURNAL OF AGRICULTURAL AND FOOD CHEMISTRY
ARTICLE

# Assessment of the Quality Attributes of Cod Caviar Paste by Means of Front-Face Fluorescence Spectroscopy

Diego Airado-Rodríguez,*[,†,‡] Josefine Skaret,[†] and Jens Petter Wold[†]

[†]Nofima Mat AS, Osloveien 1, N-1430 Ås, Norway, and [‡]Department of Analytical Chemistry, Sciences Faculty, University of Extremadura, Avda. de Elvas s/n, 06006 Badajoz, Spain

This paper describes the fluorescent behavior of cod caviar paste, stored under different conditions, in terms of light exposure and concentration of oxygen in the headspace. Multivariate curve resolution was employed to decompose the overall fluorescence spectra into pure fluorescent components and calculate the relative concentrations of these components in the different samples. Profiles corresponding to protoporphyrin IX, photoprotoporphyrin, and fluorescent oxidation products were identified. Sensory evaluation, TBARS, and analysis of volatiles are typical methods employed in the routine analysis and quality control of such food. Successful calibration models were established between fluorescence and those routine methods. Correlation coefficients higher than 0.80 were found for 79% and higher than 0.90 for 50% of the assessed odors and flavors. For instance, *R* values of 0.94, and 0.96 were obtained for fresh and rancid flavors respectively, and 0.89 for TBARS. On the basis of these data, it can be argued that front-face fluorescence spectroscopy can substitute all of these expensive and tedious methodologies.

**KEYWORDS: Caviar; photooxidation; protoporphyrin IX; front-face fluorescence; sensory analysis; DHS/GC-MS; TBARS**

## INTRODUCTION

The roe or the ovaries of a variety of marine fish, shellfish, and some anadromous and fresh water fish are used for food and are considered to be a delicacy in many parts of the world. The ovary is the female reproductive organ, and the roe consists of a pair of ovaries or membranous sacs that contain individual eggs held together by connective tissues. Individual fish eggs separated from the ovaries are commonly referred to as caviar. Sturgeon roe is considered to be the premium fish roe, and it is used to produce the most highly prized and valuable caviar and caviar products. Products made from the roe of salmon, herring, cod, Alaskan pollock, lumpfish, capelin, and other species are also in demand (*1*). Salted and smoked cod roe is popular in northern European countries.

The typical composition of fresh cod roe is 70−75% water, 15−26% protein, and about 1% (13−15% of dry weight) of lipids (*2*). Around 76% of total lipids are polar ones, which contain high levels of polyunsaturated fatty acids, while the rest of them are triglycerides, free fatty acids, and sterols (*3*).

Lipids are important structural and functional components in foods. They have a significant effect on quality, even when the lipid content is very small, as they are vulnerable to oxidation. Oxidation in food products is initiated by several factors such as exposure to light, presence of metal ions, enzymes, and thermal conditions (*4*). Lipid oxidation can be divided into three types: autoxidation, photooxidation, and enzymatic oxidation.

*To whom correspondence should be addressed at Nofima Mat AS. E-mail: diego.airado@nofima.no.

Photooxidation takes place either by photolytic autoxidation or photosensitized oxidation. Photolytic autoxidation consists in the production of free radicals primarily from lipids during exposure to UV light (*5*). This type of reaction proceeds by normal free radical chain reactions (*4*). However, direct interaction of UV light with lipids in foods is minimal. Photosensitized oxidation occurs in the presence of photosensitizers (*5*). These compounds can absorb visible or near-UV light to become electronically excited. Photosensitizers have two excited states: singlet and triplet. The triplet excited state has a longer lifetime and initiates oxidation. Photooxidation by a photosensitizer can proceed through type I or type II reactions. Type I reactions proceed through a free radical mechanism, while in type II reactions, the sensitizer reacts with oxygen to produce singlet oxygen, which is highly reactive. These reactions often occur at the same time, in a competitive fashion (*6*). However, at low oxygen concentrations, the type I reactions are most efficient (*7*).

As far as we know, in the literature there is a lack of information regarding the photostability and photooxidation of caviar. Also, nothing has been reported about potential photosensitizers present in caviar.

The most commonly reported methods for the analysis and characterization of caviar are based on sensory panels (*8*, *9*) and gas chromatography−mass spectrometry (GC-MS) for the analysis of fatty acids and volatile compounds. Within fatty acids, Caprino et al. (*10*) reported that palmitic acid (16:0) and oleic acid (18:1 *n*-9) were the most abundant fatty acids in caviar followed by docosahexaenoic acid (22:6 *n*-3) and eicopentaenoic (20:5 *n*-3). Regarding the analyses of volatile compounds, it is important to

 Published on Web 04/07/2010 

**Table 1.** Assayed Storage Conditions for the Calibration and Test Sets

| | calibration set | | | | | test set | | | |
|---|---|---|---|---|---|---|---|---|---|
| | light | | | darkness | | light | | | |
| storage time (days) | 0% $O_2$ (100% $N_2$) | 1% $O_2$ | 21% $O_2$ | 0% $O_2$ (100% $N_2$) | 21% $O_2$ | 0% $O_2$ (100% $N_2$) | 1% $O_2$ | 21% $O_2$ | darkness |
| 1 | 1L0 | | 1L21 | 1D0 | 1D21 | | | | |
| 4 | 4L0 | 4L1 | 4L21 | | 4D21 | | | T-4L21 | |
| 8 | | | | | | T-8L0 | T-8L1 | T-8L21 | |
| 10 | | | | | | | T-10L1 | T-10L21 | |
| 12 | 12L0 | 12L1 | 12L21 | | 12D21 | | | | |
| 15 | | | | | | | | T-15L21 | |
| 21 | 21L0 | | 21L21 | 21D0 | 21D21 | | | | |

note that, due to their low levels, traditional GC-MS is not sensitive enough for its analysis and preisolation/preconcentration steps are needed. Static and dynamic headspace methods, solid phase microextraction, supercritical fluid extraction, and simultaneous distillation−extraction (SDE) are typical strategies commonly used for the isolation and preconcentration of volatile compounds (*10*). Recently, Caprino et al. (*10*) isolated 33 volatile compounds from sturgeon caviar using SDE and identified them by GC-MS. It was found that aldehydes represented 60% of the total volatiles in the headspace. Also, *n*-alkanals, 2-alkenals, and 2,4-alkadienals were found to be responsible for a wide range of flavors in this kind of caviar. GC-olfactometry and electronic noses have also been employed to characterize the headspace of different commercially processed roe products, and 3-methyl-1-butanol and 3-methylbutanal have been identified as potential indicators of spoilage (*9*). Lastly, more advanced methodologies such as scanning electron microscopy (SEM), magnetic resonance imaging (MRI), and spectroscopy $T_1$ and $T_2$ proton relaxation techniques have been used to study structural properties and conservation states of salted caviar during storage (*11*).

There has been an increasing demand for rapid analytical methods which reflect the sensory perception of the consumer, especially for the control of complex foods such as caviar, due to the high costs connected to routine use of sensory evaluation and the lack of satisfactory instrumental methods. Fluorescence spectroscopy is emerging as a competitive technique for this purpose. It has demonstrated to be suitable for the analysis and characterization of different food systems (*12*). Fluorescence spectroscopy is a nondestructive method, characterized by its high sensitivity and specificity and also by its speed (a spectrum can be recorded in less than 1 s with a rather simple optical system and a CCD detector) and relatively low cost. It is reported to be 100−1000 times more sensitive than other spectrophotometric techniques (*13*). Classical 90° and front face are the main modalities of fluorescence spectroscopy. Classical 90° fluorescence spectroscopy is the common setup when working with transparent and diluted solutions (absorbance below 0.1). Powdered, turbid, and concentrated samples, as well as untreated food samples such as meat, fish, and dairy products, can be directly measured by means of front-face fluorescence. It consists of illuminating the surface of the sample with the excitation light and measuring the emitted fluorescence from the same surface.

Intact foods are very complex chemical systems; therefore, the fluorescence signals arising from those systems are a combination of individual signals from different intrinsic fluorophores, at the same time influenced by the physical−chemical environment of the food matrix (temperature, pH, color, etc.). Chemometrics is a necessity to handle these complex fluorescence signals. A great number of chemical compounds can be measured under this methodology (front-face fluorescence + chemometrics), enabling semifingerprinting of intact samples, which allows continuous and nondestructive analysis of products during processing (*12*). Front-face fluorescence spectroscopy has earlier demonstrated to be a suitable technique to determine the extent and distribution of lipid oxidation in different food matrices (*14*−*17*).

The aim of this work was to study the fluorescence behavior of cod caviar paste, to reach a better understanding of the main fluorophores in this food matrix and their relation to sensory properties, concentrations of volatiles, and traditional rancidity measurements (e.g., TBARS). Different chemometric techniques were used to analyze the spectra and to establish the relation between fluorescence spectra and the reference methods.

## MATERIALS AND METHODS

**Materials.** A homogeneous batch of 20 kg of cod caviar paste was provided by Mills (Mills DA, Oslo, Norway). When received, it was packaged under vacuum and kept in darkness at 4 °C.

For the experiment, 250 g aliquots of caviar paste were placed in 195 × 132 × 25 mm thermoformed trays (Jihå Plast AB, Karlskoga, Sweden) made of A-PET/PE sheet (Wipak Oy, Nastola, Finland). The trays were sealed with a laminate film based on oriented polyester, Biaxer 65 XX HFP AF (Wipak Oy, Nastola, Finland; $O_2$ transmission rate of 5 $cm^3$/24 h at 23 °C, 50% relative humidity) with a 511VG tray-sealing machine (Polimoon, Kristiansand, Norway). The gas in all the packages was $N_2$ with traces of $O_2$ (0.03 ± 0.03%). Once the samples were packed, small holes were opened in the film, to let air in, in the case of samples to be stored in the presence of 21% $O_2$. For the preparation of samples to be stored with 1% $O_2$ in the headspace, air was injected through a septum with a syringe up to the target $O_2$ concentration. Measurements of the concentration of $O_2$ in the headspace were made with an $O_2$/$CO_2$ analyzer (CheckMate 9900 O2/CO2, PBI-Dansensor A/S, Denmark). All trays were wrapped in one layer of transparent plastic film (Clingfilm, Toro, Norway) to avoid the loss of humidity.

**Experimental Design.** An experimental design including storage time, light exposure, and $O_2$ concentration in the headspace was created in order to obtain a large but relevant span in quality properties of cod caviar paste. Three different atmospheres were employed for the storage of the samples (anaerobic conditions with 100% $N_2$, 1% $O_2$, and 21% $O_2$). Some samples were exposed to light, while others were stored in the dark. The storage design and conditions for the calibration and test sets of samples are summarized in **Table 1**. A code was assigned to each sample, indicating the days of storage, the presence (*L*) or absence (*D*) of illumination during storage, and the concentration of $O_2$ in the headspace (**Table 1**). The codes employed in this table will be further used to identify the samples throughout the paper. The two trays containing 250 g of cod caviar paste and a third one containing two sample cuvettes filled up with cod caviar paste were stored under each condition detailed in **Table 1**. The caviar paste in the trays was used for sensory evaluation, TBARS, and volatile compounds analysis, while caviar paste in the cuvettes was directly employed for the fluorescence measurements. Thus, the calibration and test sets were made up by 32 and 14 trays of caviar paste and 32 and 14 cuvettes, respectively. The test set was generated and measured 6 weeks after the calibration set, with the objective of testing the performance of the model in the time.

The light exposure was performed in a cold-storage chamber at 4 °C with fluorescent light tubes (Osram L 58W/954 Lumilux de Luxe-Daylight) placed vertically at a distance of approximately 9 cm from the trays. Trays were randomly moved during the exposure period, in order to assess an equal illumination for all of them.

**Table 2.** Definition of Each Sensory Attribute

| kind | sensorial attribute | description |
|---|---|---|
| odors | acid | an acidic odor of vinegar |
| | sweet | odor of sweet (sugar) |
| | fresh | related to freshness, sour/sweet odor/odor of fresh sea |
| | smoke | odor of smoke |
| | rancid | rancid odor (grass, hay, candle, paint) |
| visual appearance | color hue | location of the color, measured on the surface of the sample, in the NCS color circle; yellow/red Y40R to yellow/red Y60R |
| | color strength | chromaticity; degree of pure color vs white/black on the surface of the sample |
| | whiteness | black and/or pure color to white color (NCS system); measured on the surface of the sample |
| | gloss | gloss assessed on the surface |
| | firmness | firmness assessed when stirring the sample |
| flavors | acid | an acidic flavor of vinegar |
| | sweet | the basic taste sweet (sugar) |
| | fresh | flavor of freshness, sour/sweet flavor |
| | bitter | the basic taste bitter (caffeine) |
| | salt | the basic taste salt (NaCl) |
| | metallic | flavor of metal |
| | smoke | flavor of smoke |
| | fish oil | related to fish oil |
| | rancid | rancid flavor (grass, hay, candle, paint) |
| texture | juiciness | surface textural attribute which describes the perception of water/moist absorbed by or released from the sample after 4−5 chewings |
| | granularity | geometrical textural attribute relating to the perception of the size and shape or particles in a product |
| | fatness | surface textural attribute relating to the perception of the quantity of fat in the product (mouth feel) |
| | creamy | a creamy sensation of the sample |
| aftertaste | aftertaste | the intensity of aftertaste 30 s after spitting out the sample |

**Sensory Analysis.** Sensory analysis is a scientific discipline that applies principles of experimental design and statistical analysis to the use of human senses (sight, smell, taste, touch, and hearing) for the purposes of evaluating consumer products. The discipline requires panels of human assessors, on whom the products are tested, and recording the responses made by them.

It has been shown that sensory analysis is more sensitive to attributes of photooxidation in, for example, dairy products than instrumental methods traditionally used for measurement of oxidation (*15*). The instrumental methods measure more specific compounds, but as long as these are not relevant to sensory perception, or are of too poor sensitivity, they are not very helpful.

The sensory evaluation was performed by a trained sensory panel at Nofima Mat AS using descriptive sensory profiling according to Lawless and Heymann (*18*) and ISO standards (*19*). The sensory panel consisted of 10 selected and independent assessors (*20*) and took place in a purpose-built sensory laboratory (*21*). Prior to the analysis, the panel was trained in the definition and intensities of the chosen attributes, using caviar paste with varying sensory properties (samples 1D0 and 21L21 for the calibration set and a fresh sample, nonexposed and packed under vacuum, and T-15L21 for the test set). The assessed sensory attributes are listed in **Table 2**, in the same order as they were evaluated by the assessors.

The samples in the trays were homogenized by stirring with a spoon. Then each assessor was served a teaspoon of each caviar paste sample on a cardboard plate. The samples were served at room temperature. The samples were served twice, and the serving order was randomized according to sample and assessor. Water and cucumber dices were provided to cleanse the palate between samples. A continuous nonstructured scale was used for evaluation of sensory attributes. Each judge evaluated the samples at individual speed on a computer system for direct recording of data (Compusense five, v. 4.6; Compusense, Inc., Guelph, ON, Canada), and their scores were transformed to numbers from 1 (= no intensity) to 9 (= high intensity). The sensory score for each sample of caviar paste was obtained by averaging the individual scores from the 10 assessors for each of the 10 subsamples. A total of 64 samples were evaluated in the calibration set, and the measurements had to be carried out over 2 days due to capacity limitation; 28 samples were evaluated in the test set, 6 weeks later.

**Front-Face Fluorescence Measurements.** Fluorescence emission spectra were measured directly on caviar paste samples. The samples were placed into sample cuvettes, which exposed a flat circular surface with a diameter of 5 cm for the measurements. An optical bench system optimized for measuring large sample surfaces was used. The samples were illuminated with 382 nm excitation light, and fluorescence emission spectra were measured in the range of 410−750 nm. 382 nm was selected as the excitation wavelength, as it has earlier been shown to give good results on lipid oxidation products in different food matrices (*14*−*17*). The excitation light was generated by a 300 W xenon light source (Oriel 6258; Oriel Corporation, Stratford, CT) and passed through a 10 nm bandwidth interference filter (Oriel 59920). The light was directed onto the samples at an angle of approximately 45°. The spectra were collected by an imaging spectrograph (Acton SP-150; Acton Research Corp., Acton, MA) connected to a sensitive charge-coupled device (CCD camera) (Roper Scientific NTE/CCD-1340/400-EMB; Roper Scientific, Trenton, NJ). A cutoff filter at 400 nm (Melles Griot 03FCG049; Melles Griot, Rochester, NY) was positioned in front of the spectrograph slit to suppress the excitation light reflected from the sample. The exposure time was 3 s for all spectroscopic measurements, which turned out to be a good compromise between camera sensitivity and avoidance of photodegradation of photosensitizers by the powerful excitation light. The temperature of the samples was around 5 °C. Two spectra were collected from each sample, and the average was used for further analysis. The illumination was not perfectly homogeneous; therefore, samples were rotated 90° between the two exposures. The spectrograph and detector were controlled by the software WinSpec 1.4.3.4 (Roper Scientific). The spectra were smoothed by a moving average with a window of 9 points before analysis.

**Dynamic Headspace/GC-MS Analysis of Volatile Compounds.** Volatile compounds were analyzed by a dynamic headspace method previously published by Olsen et al. (*22*). Caviar paste (10 g) was weighed into Erlenmeyer flasks (500 mL). 2 $\mu$L of ethyl heptanoate (> 99%, Sigma-Aldrich Chemie GmbH, Steinheim, Germany) in methanol (400 $\mu$g/mL) (p.a., Merck GmbH, Darmstadt, Germany) were added into the flasks as an internal standard. The samples were placed in a water bath, heated to 70 °C, and purged with 100 mL/min of purified nitrogen through a Drechsel-head for 20 min. Volatiles were adsorbed on Tenax GR (mesh size 60/80, Alltech Associates Inc., Deerfield, IL). Water was removed from the absorber by $N_2$ flushing (50 mL/min) for 5 min in the opposite direction of sampling. Trapped compounds were desorbed at 280 °C for 5 min in a Markes Ultra, UNITY Thermal desorption unit (Markes International Ltd., Llantrisant, U.K.) and transferred to an Agilent 6890 GC system (Agilent, Palo Alto, CA) with an Agilent 5973 mass spectrometer (a quadrupole) operated in electron ionization (EI) mode at 70 eV. The compounds were separated on a DB-WAXetr column (J&W Scientific, Agilent) (0.25 mm i.d., 0.5 $\mu$m film, 30 m) with helium (99.9999%) as carrier gas. The temperature program started at 30 °C for 10 min, increased 1°/min to 40 °C, 3°/min to 70 °C, and 5°/min to 230 °C.

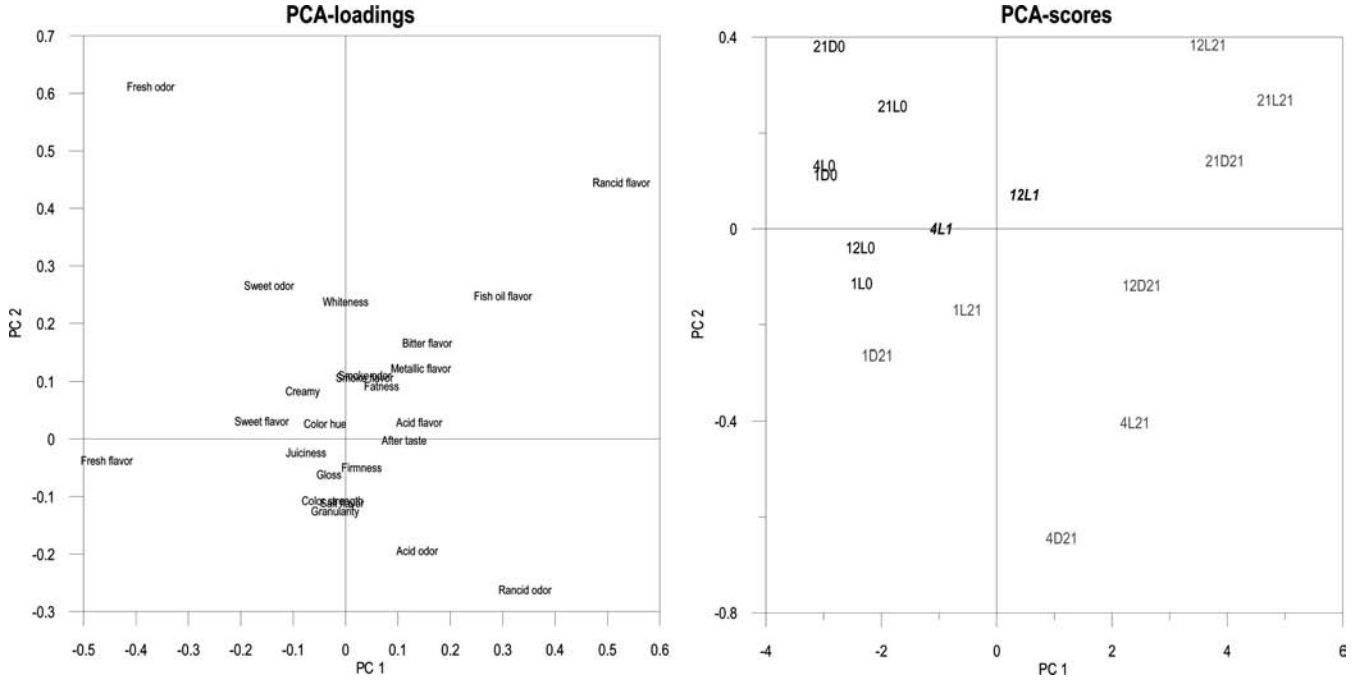


**Figure 1.** Principal component analysis loadings and scores for the first two PCs on the assessed sensorial attributes on the calibration sample set. In the scores plot, samples are grouped according to the percentage of oxygen in the headspace.

The final holding time was 5 min. Integration of peaks and tentative identification of compounds were performed with an HP Chemstation (G1701CA version C.00.00, Agilent Technologies), the Wiley 130K Mass Spectral Database (HP 61030A MS Chemstation), and the NIST Mass Spectral Library (version 2.0 2005, U.S. Secretary of Commerce/Agilent). The concentrations of the individual volatiles were calculated as ng of volatile/g of sample, on the basis of the internal standard. No corrections were made for the different recoveries of the various volatiles; therefore, the calculated concentrations were regarded as semiquantitative only. The analysis was performed in duplicate for all samples.

**2-Thiobarbituric Acid Reactive Substances (TBARS Values).** The 2-thiobarbituric acid reactive substances (TBARS) assay was performed by a method slightly modified from that proposed by Buege and Aust in 1978. Duplicate samples of caviar paste (0.10 g) were mixed with 3.0 mL of stock solution containing 0.375% of 2-thiobarbituric acid (TBA) (Sigma Chemical Co., St. Louis, MO), 15% trichloroacetic acid (TCA) (Merck KGaA, Germany), and 0.25 N HCl. The mixture was vortexed and heated for 10 min in a boiling water bath (100 °C) to develop a brownish color. Later, it was cooled in tap water and centrifuged at 5500 rpm for 25 min. A 0.50 mL aliquot of the supernatant was transferred into the measurement cell and further diluted with 2.50 mL of ultrapure water. The absorbance was spectrophotometrically (Ultraspec 3000, Pharmacia Biotech, Cambridge, U.K.) measured at 532 nm, against a blank which contained all the reagents, minus the caviar paste. The absorbance measurements were normalized by dividing them by the exact weight of cod caviar paste taken in each case. The normalized $A_{532\ nm}$ values, further referred to as the TBARS index, were employed to look for correlations with the fluorescence spectra.

**Data Analyses.** Multivariate curve resolution (MCR) was applied on the whole collection of fluorescence spectra (calibration and test sets) to extract pure spectra and concentration profiles from the fluorescence data matrix. A non-negativity constraint was applied in the spectra and concentration modes, in order to obtain a realistic solution. The algorithm for MCR has been previously described in detail by Tauler (*23*) and Tauler et al. (*24*). MCR was carried out with the software The Unscrambler (v. 9.8, Camo AS, Oslo, Norway).

Partial least-squares regression (PLSR) (*25*) was used for making calibrations between fluorescence spectra and sensory-assessed attributes of caviar paste, DHS/GC-MS, and TBARS. The optimal number of PLSR factors of the calibration models was determined by segmented cross-validation, leaving out the two replicates corresponding to the same storage conditions, in the same segment. The predicted value for each sample, $\hat{y}_i$, was compared with the reference value, $y_i$ (sensory, DHS/GC-MS, or TBARS). The multivariate correlation coefficient ($R$), which describes the relationship between the measured and the predicted values of the $y$ variable(s), and the prediction error of the regression model, expressed as root-mean-square error of cross-validation (RMSECV), were used to evaluate the models. RMSECV is defined as

$$\mathrm{RMSECV} = \sqrt{\frac{1}{N}\sum_{i=1}^{N}(y_i - \hat{y}_i)^2}$$

where $i$ denotes the samples from 1 to $N$.

The calibration models were employed for the prediction of reference values for the sensorial attributes, as well as TBARS of the test set samples. Model performance was reported as the root-mean-square error of prediction (RMSEP), calculated exactly as RMSECV ($\hat{y}_i$ being a result of prediction and not cross-validation), and the multivariate correlation coefficient ($R$). PLSR was performed with the software The Unscrambler (v. 9.8, Camo AS, Oslo, Norway).

## RESULTS AND DISCUSSION

**Sensory Analysis. Figure 1** shows the loadings from the first and second PCs of a principal components analysis (PCA) carried out on the assessed sensorial attributes for the samples included in the calibration set. These PCs explain 96% and 1% of the total variance, respectively. The score plot for PC1 vs PC2 is also shown in the same figure, and the 16 samples integrating the calibration set can be identified in this "map of samples", grouped according to the percentage of oxygen in the headspace. Attributes related to the visual appearance and granularity, as well as smoke odor and flavor and salt flavor, are distributed along the PC2 axis; however, all of them lie close to the origin of PC1. In other words, these attributes did not contribute, to a high degree, to the whole variation of the system. The span of the distribution of attributes in this variables map is constituted mainly by the fresh odor and flavor on the left and the rancid odor and flavor on the right. Sweet odor and flavor, as well as creamy and juiciness, are located at the left side of the plot, in the same direction as freshness-related attributes, and are also desired attributes in

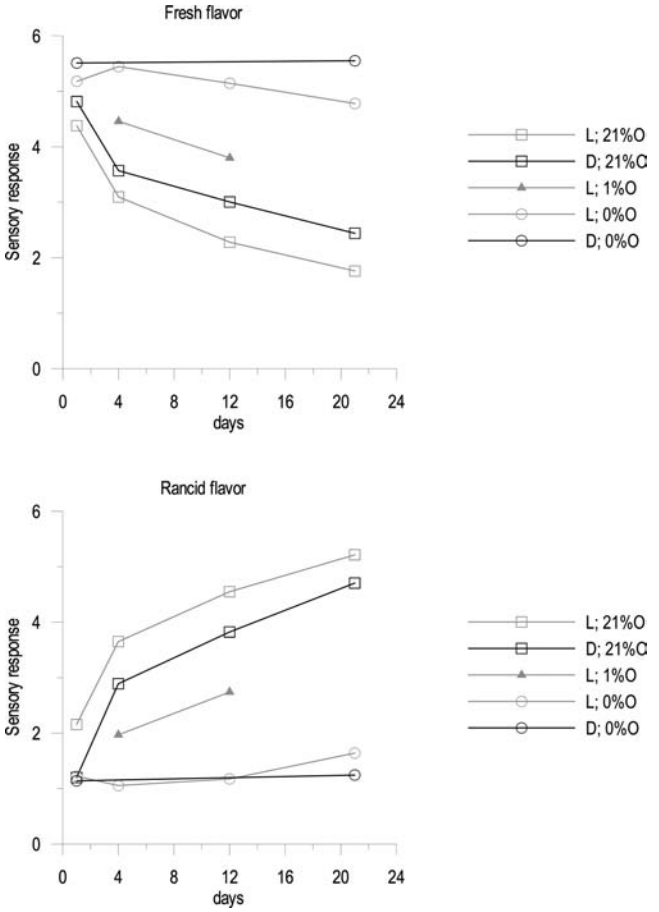


**Figure 2.** Development of rancid and fresh flavor intensities for caviar paste, stored under different conditions.

caviar paste. On the other hand, aftertaste, metallic, bitter, and fish oil flavors, as well as acid odor and flavor, are located at the right side, as they are rancidity-related attributes. Thus, PC1 represents the freshness/desirability of caviar paste in increasing sense from right to the left.

The samples in the score plot are positioned in accordance to the properties in the loading plot. It seems to be the concentration of oxygen in the headspace, which was the most important variable affecting the position of a sample in this scores plot. Samples packed in absence of oxygen are located in the left side of the sample map. The position on PC1 for these samples seems to be independent of the presence or absence of light and the time of storage. On the other hand, samples packed in the presence of air are located at the right side. Samples 1D21 and 1L21 are an exception, as 1 day of storage is not enough to make the undesired attributes noticeable. However, it is noteworthy how the presence of light can locate 1L21 to the right of 1D21. Finally, regarding the samples packed in the presence of 1% of oxygen, they are close to the origin, the sample stored for 12 days is located at the right side, and the sample stored for 4 days at the left side, as expected.

The development of fresh and rancid flavors in caviar paste, stored under different conditions, is shown in **Figure 2**, as representative positive and negative attributes, respectively. A decrease in the freshness and an increase in the rancidity with time is observed for the samples stored in the presence of air, independent of the lightening. The freshness of the sample stored in the dark under nitrogen is kept over 21 days, and a slight decrease is observed in the case of the sample stored under nitrogen in the presence of light. This graph will be further

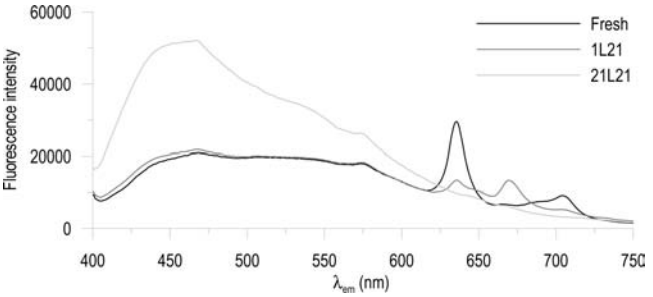


**Figure 3.** Fluorescence emission spectra ($\lambda_{ex}$ = 382 nm) corresponding to a fresh caviar paste sample (black line) and two samples stored in the presence of 21% of $O_2$ and exposed to light for 1 (1L21; dark gray line) and 21 days (21L21; light gray line).

discussed more deeply and related to the fluorescent properties of caviar paste.

**Fluorescence Spectroscopy.** In **Figure 3**, the fluorescence emission spectra of three samples stored under different conditions are shown. The peaks at 635 and 705 nm are attributable to protoporphyrin IX (PpIX). Porphyrins are a large group of organic compounds, which consist of four pyrrole rings joined by methene bridges. The fluorescence emission spectra of PpIX is characterized by a sharp peak at 635 nm and a broader one at 705 nm (*26*). The fluorescence properties of PpIX have also been assayed by spiking experiments in different food matrices, such as cheese (*27*), butter (*28*), and pork meat (*14*), corroborating the position of both emission peaks in the presence of complex matrices. PpIX has been also nondestructively quantified in butter by front-face fluorescence (*28*). This compound has been referred to as a photosensitizer and potential initiator of photooxidation in meat and in products containing vegetables (*29*), as well as in dairy products (*27*). Porphyrin-type dyes are also widely used as photosensitizers in the photodynamic therapy (PDT) of cancer (*26*). PpIX could be highlighted in the emission spectrum of caviar paste by exciting at 407 nm, which corresponds to the maximum of the Soret band (*26*). However, due to the apparently high concentrations of PpIX in cod caviar paste, it was possible to employ 382 nm as a compromise excitation wavelength to monitor in a single scan both the oxidation products and the photosensitizer concentration.

In the spectrum corresponding to the sample stored for 1 day in the presence of air and light (1L21; **Figure 3**), another peak is observed centered at 670 nm, which can be assigned on the basis of bibliographic data to the main photoproduct of PpIX, called photoprotoporphyrin (PPp) (*26*, *30*). Phototransformations of porphyrins are well documented in the literature related to the field of PDT (*26*). Such transformations normally involve decay (photobleaching) of absorbance and fluorescence and result in formation of photoproducts. Inhoffen et al. (*31*) were the first to describe phototransformations of PpIX, mainly as transformations from porphyrin-like to chlorin-like molecules. Chlorins consist of three pyrrole rings and one pyrroline ring joined by methene bridges. According to the literature, the so-called photoprotoporphyrin is a mixture of two clorin-type hydroxyaldehyde isomers (*31*, *32*), formed by the action of light on PpIX. As previously reported by Ericson et al. (*33*), PPp presents a fluorescent emission maximum at 670 nm and an excitation maximum at 428 nm. The chlorin-like molecule PPp has also been reported as a photosensitizer itself (*29*).

The broad fluorescence band observed in the region from 410 to 500 nm, very intense especially in the sample 21L21, arises from different stable fluorescent oxidation products: among them, products formed by the reaction of unsaturated aldehydes

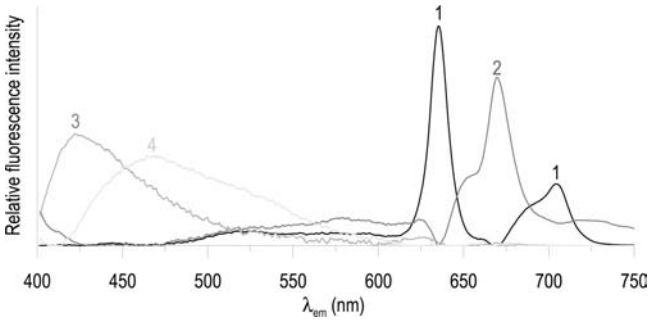


**Figure 4.** Spectral profiles of the estimated pure components by means of MCR.

with proteins (*34*). The peak at 470 nm has been associated with lipid oxidation products, and it is common to different food matrices, such as minced turkey, pork, and cod meat (*34*), chicken meat (*16*), salmon pâté (*35*), and dairy products (*15*, *17*), among others. However, the individual fluorophores responsible for the signals in this region are not certain yet. A possible way to identify some of them could be to match fluorescence with results from liquid chromatography or some other separation technique and search for correlations.

MCR was applied in an effort to separate the different true spectral components. This would aid the interpretation of the system and the observed variations. MCR was applied on the whole collection of fluorescence spectra (calibration + test sample sets). Four components were found to explain the structure of the fluorescence data set. The obtained spectral profiles corresponding to pure components are presented in **Figure 4**. Component 1 is clearly identified as PpIX, with its two characteristic emission maxima at 635 and 705 nm. Component 2, with a maximum at 670 nm and a shoulder at 654 nm, is attributable to PPp. A small valley is observed in this spectral profile at 635 nm, which probably corresponds to a mathematical artifact just to compensate the sharp and intense peak corresponding to PpIX. Oxidation products are represented by components 3 and 4, with maxima centered at 423 and 470 nm, respectively. Component 4 is related to fluorescent lipid oxidation products resulting from the reaction of aldehydes with proteins or amino acids (*34*,*36*). Also, oxidation products with an emission maximum at 425 nm ($\lambda_{ex}$ = 350 nm) have been reported, for example, in oxidized soybean flour (*37*). On the basis of a study on the interaction between oxidizing soybean oil and soy proteins (*38*), it can be asserted that such products are Schiff base structures, likely arising from the interaction between TBA-reactive substances and free amino groups of proteins. The structure of these fluorophores, cross-links, and borohydride-reducible functions produced in proteins by lipid oxidation were elucidated in the 1990s by Kikugawa et al (*39*).

The relative concentrations of the four fluorescent components in all samples were also estimated by MCR. The evolution of the concentrations of components 1 (PpIX), 2 (PPp) and 4 (fluorescence oxidation products), under different storage conditions, is presented in **Figure 5**. The evolution of component 3 was not included in the figure, as it covaried closely with component 4. It is very interesting to carry out the analysis of **Figure 5** together with **Figure 2**, to relate the variation of sensory and fluorescence properties of cod caviar paste.

Cod caviar paste stored under vacuum in the darkness was stable toward photooxidation during the 21 days, since neither bleaching of PpIX nor development of oxidation products was observed during this period. Sensorial evaluation copes well with this fluorescent behavior, since no changes in the fresh and rancid flavors were detected during the whole period.

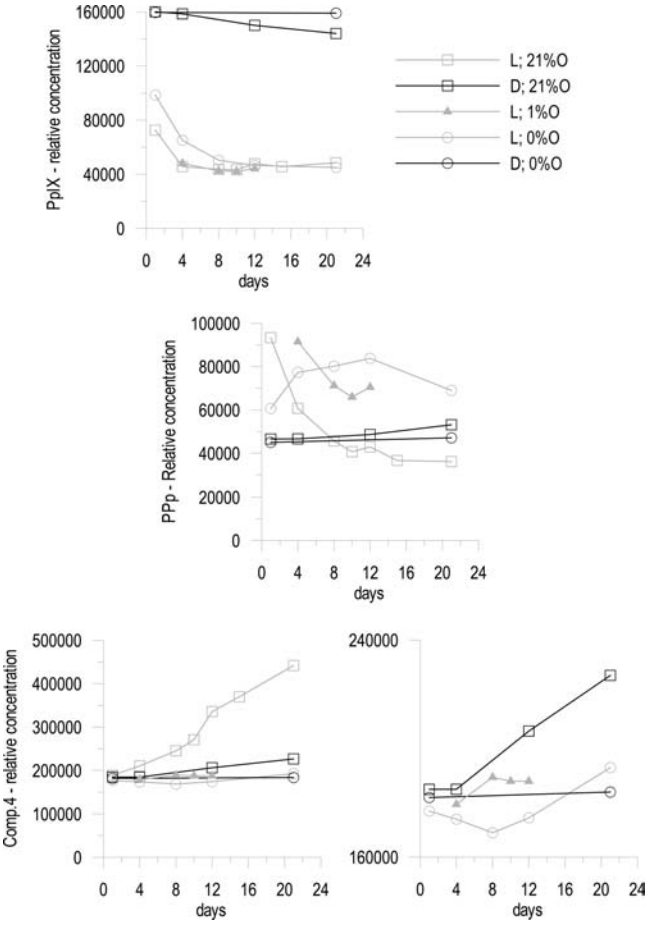


**Figure 5.** Evolution of the relative MCR-estimated concentrations of fluorescence components 1 (PpIX; top), 2 (PPp; middle), and 4 (oxidation products, bottom) under different storage conditions. An enlargement has been included for the evolution of component 4.

Regarding the sample stored in the darkness in the presence of 21% of $O_2$, a slight decrease in the PpIX concentration was observed, since this compound could be acting as an antioxidant under these storage conditions. The concentration of oxidation products increased from the fourth day, although to a much lesser extent than in the case of the sample stored in 21% $O_2$ in the presence of light. However, the sensory panel was able to detect the decrease in freshness and the increase in the rancidity for this sample, immediately from the first day of storage, making the samples stored in 21% $O_2$ in the presence and absence of light very similar with regard to the evolution of these sensory attributes. This late detection of the fluorescent lipid oxidation products in comparison with the changes in the sensory properties has also been observed, for example, in butter exposed to light (*15*). An autoxidation process, due to the exposure of unsaturated fatty acids to oxygen, was probably responsible for the loss of freshness. It consists of an autocatalytic chain reaction and proceeds through a free-radical chain reaction mechanism involving three stages: initiation, propagation, and termination. Autoxidation can be initiated by trace metals and peroxides or hydroperoxides present as natural components in foods (*4*).

In the case of samples exposed to light in the absence of $O_2$, a total photobleaching of PpIX is observed after 8 days. Also, an increase in the PPp concentration is observed during the first 12 days, which indicates a porphyrin-like to chlorin-like transformation induced by light, as the first step of the changes induced by light in this system. However, it seems that PpIX by itself does

**Table 3.** Results from Partial Least-Squares Regression (PLSR) for Some Sensory-Assessed Attributes and TBARS against Fluorescence[a]

| | | calibration ($N = 32$) | | | | prediction ($N = 14$) | | |
|---|---|---|---|---|---|---|---|---|
| kind | sensorial attribute | $R$ | #F | RMSECV | $Y_{cal}$ range | $R$ | RMSEP | $Y_{test}$ range |
| odor | acid | 0.84 | 4 | 0.21 | 3.1−4.1 | 0.91 | 0.32 | 3.6−4.2 |
| | sweet | 0.89 | 7 | 0.18 | 3.3−4.4 | 0.82 | 0.29 | 3.4−4.1 |
| | fresh | 0.83 | 4 | 0.56 | 2.5−5.5 | 0.90 | 0.40 | 3.2−5.3 |
| | smoke | 0.47 | 7 | 0.16 | 4.3−4.8 | | | |
| | rancid | 0.84 | 4 | 0.50 | 1.0−3.7 | 0.91 | 0.30 | 1.1−3.0 |
| visual appearance | color hue | 0.52 | 1 | 0.13 | 4.5−5.2 | | | |
| | color strength | 0.62 | 1 | 0.08 | 4.7−5.2 | | | |
| | whiteness | *-0.27* | 1 | 0.13 | 4.6−5.0 | | | |
| | gloss | 0.13 | 1 | 0.16 | 5.3−5.7 | | | |
| | firmness | 0.36 | 1 | 0.13 | 5.0−5.5 | | | |
| flavor | acid | 0.93 | 4 | 0.14 | 3.3−4.5 | 0.87 | 0.43 | 3.7−4.6 |
| | sweet | 0.96 | 6 | 0.12 | 3.3−4.5 | 0.92 | 0.27 | 3.5−4.2 |
| | fresh | 0.94 | 5 | 0.41 | 1.8−5.6 | 0.97 | 0.37 | 2.8−5.6 |
| | bitter | 0.96 | 6 | 0.13 | 4.6−6.1 | 0.95 | 0.14 | 4.6−5.6 |
| | salt | 0.57 | 7 | 0.077 | 5.8−6.1 | | | |
| | metallic | 0.93 | 7 | 0.15 | 4.1−5.3 | 0.97 | 0.090 | 4.2−5.2 |
| | smoke | 0.76 | 7 | 0.12 | 4.2−4.7 | 0.50 | 0.62 | 4.9−5.4 |
| | fish oil | 0.95 | 6 | 0.26 | 2.6−5.0 | 0.93 | 0.24 | 3.4−4.7 |
| | rancid | 0.96 | 6 | 0.39 | 1.1−5.2 | 0.97 | 0.28 | 1.4−4.7 |
| texture | juiciness | 0.82 | 4 | 0.12 | 4.5−5.2 | 0.95 | 0.18 | 4.4−5.4 |
| | granularity | 0.25 | 1 | 0.11 | 4.7−5.1 | | | |
| | fatness | 0.78 | 4 | 0.14 | 4.5−5.3 | 0.91 | 0.13 | 4.6−5.3 |
| | creamy | 0.76 | 4 | 0.16 | 4.5−5.3 | 0.80 | 0.12 | 4.5−5.0 |
| aftertaste | aftertaste | 0.89 | 7 | 0.14 | 5.3−6.3 | 0.97 | 0.15 | 5.3−6.3 |
| TBARS index | | 0.89 | 2 | 0.033 | 0.68−1.0 | 0.94 | 0.034 | 0.75−0.88 |

[a] $R$ gives the correlation coefficient, #F gives the number of PLSR factors used in the model, RMSCV is the root mean square error of cross-validation, and RMSEP is the root mean square error of prediction.

not act as a photosensitizer in this case, as no increase in the concentration of the fluorescent oxidation products is observed at the eighth day compared to the start or, since very little oxygen was present under these conditions, the oxidation reactions could not proceed and create secondary oxidation products. The concentration of the fluorescent oxidation products starts growing slightly from the eighth day, which suggests that PPp is acting as a photosensitizer and giving rise to oxidation reactions via a type I mechanism. When all the PpIX has been bleached, a decrease in the PPp concentration is observed, as no more PPp is being generated. The PPp is then being degraded and probably acting as a photosensitizer. It seems that, under this anaerobic atmosphere, PPp is preferred to PpIX as a photosensitizer and the initial phototransformation PpIX/PPp precedes the oxidation photoreactions; however, the photooxidation does not take place to a great extent. These results are in good accord with the assessment made on the rancidity and freshness by the sensory panel, as a slight increase in the rancid flavor is detected after the 12th day; on the other hand, with regard to the fresh flavor, a slight decrease was observed from the fourth day. It can be concluded that, even with light, very little oxidation occurs. PpIX was degraded, but this did not lead to the formation of secondary oxidation products, affecting sensory properties minimally, or the fluorescence. Similar results were found, for example, in a study carried out by Moan and Sommer (*40*), where cells were incubated with hematoporphyrin derivative and exposed to light at different oxygen concentrations. No photoinactivation was observed when the atmosphere above the medium overlying the cells was pure $N_2$.

In the sample stored under light in the presence of 21% of $O_2$, the total degradation of PpIX is achieved after 4 days. Also, a continuous decrease in the concentration of PPp is observed. In this case, the concentration of fluorescent oxidation compounds increases almost linearly from the first day until the 21st one, which suggests that both PpIX and PPp acted as photosensitizers the whole storage period. A continuous, but not linear, decrease of fresh flavor and increase of rancid flavor was observed during the 21 days.

Samples under an atmosphere containing 1% of $O_2$ were assayed only between days 4 and 15. PpIX was completely bleached after 4 days of light exposure, and a decrease in the relative concentration of PPp was also observed from this day. The concentration of the fluorescent oxidation products increased slightly between the fourth and the eighth days, and then it kept constant until the 12th day. No further conclusions could be made, due to the small magnitude of the changes and the short assayed period of time.

In these last two cases (21 and 1% $O_2$), both type I and type II reactions could take place simultaneously in a competitive fashion (*6*).

Finally, we will remark that there is a controversy in the literature regarding the necessity of oxygen for the formation of PPp from PpIX: initially, it was proposed that PPp was formed from PpIX via photooxidation (*32*). Some years later, some evidence showed that photoproduct formation was different in different media (*41*, *42*). Later, photoproduct formation was observed under conditions with a depleted oxygen concentration (*43*). The degradation of PpIX and hematoprotoporphyrin has been shown to take place, despite removal of the oxygen through $N_2$ bubbling (*44*, *45*), and photoproduct is formed (*44*). Ericson et al. assessed in 2003 that the presence of oxygen was necessary to observe the formation of PPp (*33*). They concluded that the formation of PPp is a photo-oxidation process and that no photobleaching takes place in the absence of oxygen, and the build-up of photoproduct at 670 nm is completely abolished when the sample is deoxygenated by the freeze−pump−thaw method. When comparing their results to the studies carried out by $N_2$ bubbling, these authors argue that $N_2$ bubbling does not completely remove the oxygen from the solution. However, it is important to highlight that these authors worked in DMF

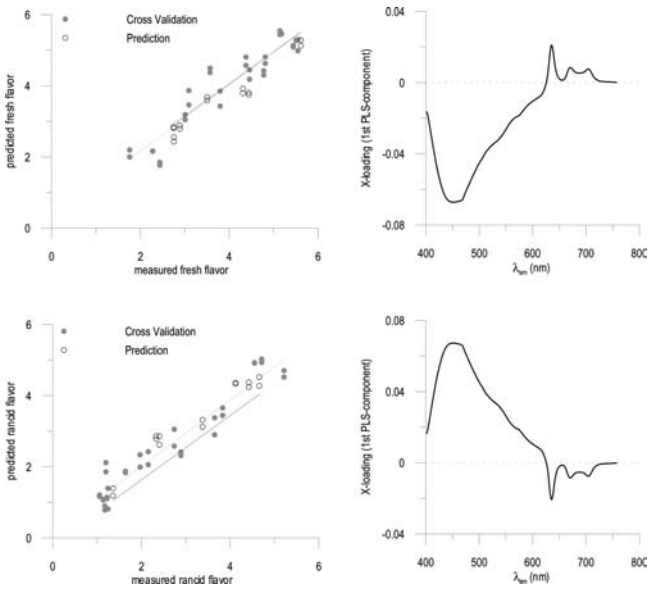


**Figure 6.** Predicted vs measured sensory assessed fresh (top) and rancid (bottom) flavors by calibration models based on fluorescence spectra and their respective X loadings for the first PLS component.

solution and the results are not always able to be extrapolated to real food matrices. In our case, the fact is that the formation of PPp was observed in all the light-exposed samples, even in the absence of oxygen, as described above. The rate of formation, however, decreases with decreasing oxygen concentration. Also, concentrations of $O_2$ less than 0.03 could not be assessed with the employed packaging gases, and this could be enough to start the photobleaching.

**Correlation between Sensory Analysis and Fluorescence.** The fluorescence spectra from untreated cod caviar paste were correlated with its sensory properties using PLSR (**Table 3**). There was a high correlation between fluorescence and every assessed odor and flavor, except for the smoke odor and the smoke and salt flavors, which is likely due to the narrow span within the scores given by the judges for these attributes (0.5, 0.5, and 0.3 units, respectively). Low correlation was found between fluorescence spectra and attributes related to the visual appearance. Granularity was also poorly correlated with the fluorescence. But apart from these single attributes, the rest of them were highly correlated with fluorescence, and successful predictions could be made.

**Figure 6** shows the predicted vs measured values for the assessed fresh and rancid flavors. In the graph related to the rancid flavor, a slight offset is observed between the lines corresponding to the cross-validation and prediction, due to a slight drift in the sensory panel. On the basis of these data (as well as in the data summarized in **Table 3**), it can be stated that front-face fluorescence can substitute for a sensory panel, in terms of sensitivity and accuracy. Making conclusions based on the behavior of regression coefficients as a function of wavelength might be very complex (*46*). However, it is tempting to look at the profiles corresponding to the X-loadings for the established PLSR models (**Figure 6**) and try to match them with characteristic spectral features of caviar. The shape of the curve corresponding to the X-loading for the first component in the PLSR model for rancid flavor (87 and 65% explained variance in X and Y blocks, respectively), for wavelengths below 550 nm, resembles the typical fluorescence arising from stable oxidation products (MCR − pure components 3 and 4). On the other hand, the shape of that curve for wavelengths above 625 nm corresponds to a mirror image of the typical emission peaks of PpIX (635 and 705 nm) and PPp (670 nm). The inverse behavior is observed for the curve corresponding to the X loading for the first component in the PLSR model for fresh flavor (87 and 65% explained variance in X and Y blocks, respectively). This indicates that the reduction in freshness and increase in rancidity was related to the breakdown of PpIX and PPp (both photosensitizers) and the subsequent generation of fluorescent lipid oxidation products (fluorescing below 550 nm). The same trends as for the rancid flavor is observed for rancid and sour odors, bitter, metallic, fish oil, and acid flavors, aftertaste, and fatness, which indicates that all of them are negative and undesirable sensorial attributes. On the other hand, fresh and sweet odors, sweet and salt flavors, and juiciness show the same behavior, in terms of X loading for the first component in their respective PLSR models, as fresh flavor; thus, these could be considered as desirable sensorial attributes for cod caviar paste. Nevertheless, apart of their denomination as positive or negative sensorial attributes, all of them have to be present in the product, in the right extension, as fully ripened roe typically have a balanced mixture of sweet, salt, bitter, and whey-like flavors (*9*).

Finally, it is also important to remark that a positive correlation is observed between the fluorescence at 635, 670, and 705 nm, and the color intensity, which corroborates that the bleaching of PpIX implies a loss of color in the sample.

**TBARS.** A PLSR model based on fluorescence spectra (X) and the TBARS index (Y), of the samples corresponding to the calibration set, was constructed (**Table 3**). TBARS values of the samples belonging to the test set were successfully predicted (**Table 3**) on the basis of the constructed model. Thus, it can be assessed that front-face fluorescence spectroscopy could serve as a rapid substitute for the tedious, time-consuming, and chemical TBARS method. In spite of this high correlation between fluorescence spectroscopy and TBARS results, one has to be careful when comparing these two methods, due to the high specificity of fluorescence and the lack of it in the case of TBARS.

Regarding the correlation between TBARS and sensory properties, it can be pointed out that negative correlations ($r$ values ranging between $-0.52$ and $-0.70$) were found between TBARS indexes and sweet and fresh odors, color hue and strength, sweet and fresh flavor, juiciness and creamy; on the other hand, TBARS was shown to be positively correlated ($0.58 \leq r \leq 0.72$) with acid and rancid odors, acid, bitter, metallic, fish oil, and rancid flavours, fatness, and aftertaste.

It is reported that Schiff bases arising from the interaction between TBA-reactive substances and free amino groups of proteins fluoresce at 425 nm (*38*). Thus, some correlation should be expected when plotting the MCR-predicted concentrations for component 3 vs the TBARS index values. In fact, the corresponding 2D scatter plot shows a correlation coefficient ($r$) of 0.89 (including both calibration and test samples), which is in accordance with the starting hypothesis of Liang (*38*).

**Volatile Components.** The main volatiles previously reported in caviar by Caprino et al. (*10*) were successfully detected and baseline-resolved, with the employed DHS/GC-MS method.

Correlations (PLSR) between the concentrations of volatiles and fluorescence spectra of caviar intact samples were investigated. Not many volatiles correlating with the fluorescence were found. The only good models were constructed for pentanal ($R$ = 0.84), benzaldehyde ($R$ = 0.74), ($Z$)-2-penten-1-ol ($R$ = 0.81), and thyazole ($R$ = 0.72). It is quite logical, to a certain extent, not to find many matches, as the oxidation compounds contributing to the fluorescence (e.g., carbonyl compounds) are normally linked to amino acids or proteins and they are not released from these Schiff bases under the conditions employed for the extraction of volatiles. For instance, an alkaline hydrolysis would be necessary to release them.

As it was said in the Introduction, 3-methylbutanal and 3-methyl-1-butanol have been reported as potential indicators of spoilage (*9*). In our experiments, an increase of the concentration of both of them, with regard to the sample 1D0, is observed under all the assayed storage conditions. Increases in the concentration of 3-methylbutanal of 190% and 141% were observed for the samples 21D21 and 21L21, respectively. With regard to 3-methyl-1-butanol, increments of 100% and 50% were observed for 21D21 and 21L21, respectively. In both cases, the increments observed in darkness were higher than those in the presence of light, which suggests that these compounds could be generated via autoxidation. However, in the sample 21L0, an increment of around 85% was observed for both compounds, which proves that type I reactions could also be responsible for their formation. Other volatile compounds of interest are 1-penten-3-ol and 2-methylbutanal, whose concentrations increased with storage time for the samples stored in the presence of light with both 1 and 21% of oxygen, as well as for the samples stored in the darkness in presence of 21% of oxygen.

To sum up, it has been demonstrated that the fluorescence spectra arising from untreated cod caviar paste samples are highly correlated with several important sensorial attributes. From a chemical point of view, the high level of correlation observed between a spectroscopic technique, which responds to the physical−chemical properties of the sample, and the sensorial assessment, purely based on human sensations, is noteworthy. On the basis of these results, the sensitivity and accuracy of front-face fluorescence is probably sufficient for rapid quality screening of caviar and could for routine measurements substitute a sensory panel, which nowadays is the quality control method mostly employed in commercial production. The caviar samples in this study were from the same batch. Further studies are needed to check if the methodology is still valid for sample sets with natural inherent biovariability.

## ACKNOWLEDGMENT

We thank Kari Thyholt from Mills DA (Oslo, Norway), for providing cod caviar paste samples. Dr. Annette Veberg, at Nofima Mat AS, is thanked for being helpful in the planning and execution of the fluorescence experiments. Dr. Maria Mielnik, at Nofima Mat AS, is thanked for being helpful in the development and discussion regarding the reference methods for the measurement of rancidity. Frank Lundby, Aud Spedal, and Karin Solgaard, at Nofima Mat AS, are also thanked for excellent technical assistance. The work was funded by The Norwegian Research Council (project no. 192309/I10 and 195614/V11) and The Fund for the Research Levy on Agricultural Products. D.A-R. thanks the *Junta de Extremadura* for a contract (DOE 154, 08/08/08).

## LITERATURE CITED

(1) Martin, R. E.; Carter, E. P.; Davis, L. M.; Flick, G. J. *Marine & Freshwater Products Handbook*; Technomic: Lancaster, PA, 2000.

(2) Martinsdottir, E.; Magnusson, H. *Sensory, Chemical and Microbiological Changes in Cod Roe during Ripening*; Icelandic Fisheries Laboratories: Reykjavik, Iceland, 1997.

(3) Kaitaranta, J. K.; Ackman, R. G. Total lipids and lipid classes of fish roe. *Comp. Biochem. Physiol.* **1981**, *69*, 725–729.

(4) Frankel, E. N. *Lipid Oxidation*.; The Oily Press: Davis, CA, 2005.

(5) Bradley, D. G.; Min, D. B. Singlet oxygen oxidation of foods. *Crit. Rev. Food Sci. Nutr.* **1992**, *31*, 211–236.

(6) Spikes, J. D. Photosensitization. In *The Science of Photobiology*, 2nd ed.; Smith, K.C., Ed.; Plenum Press: New York, 1988; pp 79−110.

(7) He, Y. Y.; An, J. Y.; Jiang, L. J. EPR and spectrophotometric studies on free radicals and singlet oxygen generated by irradiation of cysteamine substituted hypocrellin B. *Int. J. Radiat. Biol.* **1998**, *74*, 647–654.

(8) Cardinal, M.; Cornet, J.; Vallet, J. L. Sensory characteristics of caviar from wild and farmed sturgeon. *Int. Rev. Hydrobiol.* **2002**, *87*, 651–659.

(9) Jonsdottir, R.; Olafsdottir, G.; Martinsdottir, E.; Stefansson, G. Flavor characterization of ripened cod roe by gas chromatography, sensory analysis and electronic nose. *J. Agric. Food Chem.* **2004**, *52*, 6250–6256.

(10) Caprino, F.; Moretti, V. M.; Bellagamba, F.; Turchini, G. M.; Busetto, M. L.; Giani, I.; Paleari, M. A.; Pazzaglia, M. Fatty acid composition and volatile compounds of caviar from farmed white sturgeon (*Acipenser transmontanus*). *Anal. Chim. Acta* **2008**, *617*, 139–147.

(11) Gussoni, M.; Greco, F.; Vezzoli, A.; Paleari, M. A.; Moretti, V. M.; Beretta, G.; Caprino, F.; Lanza, B.; Zetta, L. Monitoring the effects of storage in caviar from farmed *Acipenser transmontanus* using chemical, SEM, and NMR methods. *J. Agric. Food Chem.* **2006**, *54*, 6725–6732.

(12) Christensen, J.; Nørgaard, L.; Bro, R.; Engelsen, S. B. Multivariate autofluorescence of intact food systems. *Chem. Rev.* **2006**, *106*, 1979–1994.

(13) Strasburg, G. M.; Ludescher, R. D. Theory and applications of fluorescence spectroscopy in food research. *Trends Food Sci. Technol.* **1995**, *6*, 69–75.

(14) Veberg, A.; Sørheim, O.; Moan, J.; Iani, V.; Juzenas, P.; Nilsen, A. N.; Wold, J. P. Measurement of lipid oxidation and porphyrins in high oxygen modified atmosphere and vacuum-packed minced turkey and pork meat by fluorescence spectra and images. *Meat Sci.* **2006**, *73*, 511–520.

(15) Veberg, A.; Olsen, E.; Nilsen, A. N.; Wold, J. P. Front face fluorescence measurement of photosensitizers and lipid oxidation products during photo-oxidation of butter. *J. Dairy Sci.* **2007**, *90*, 2189–2199.

(16) Wold, J. P.; Kvaal, K. Mapping lipid oxidation in chicken meat by multispectral imaging of autofluorescence. *Appl. Spectrosc.* **2000**, *54*, 900–909.

(17) Wold, J. P.; Veberg, A.; Lundby, F.; Nilsen, A. N.; Moan, J. Influence of storage time and color of light on photooxidation in cheese: a study based on sensory analysis and fluorescence spectroscopy. *Int. Dairy J.* **2006**, *16*, 1218–1226.

(18) Lawless, H. T.; Heymann, H. *Sensory Evaluation of Food: Principles and Practices*; Chapman & Hall: New York, 1998.

(19) *ISO 13299, Sensory Analysis-Methodology-General Guidance for Establishing a Sensory Profile*; International Organization for Standardization: Geneva, Switzerland, 2003.

(20) *ISO 8586, Sensory Analysis Methodology-General Guidance for the Selection, Training, and Monitoring of Assessors, Part 1: Selected Assessors*, 1st ed.; International Organization for Standardization: Geneva, Switzerland, .1993.

(21) *ISO 8589, Sensory Analysis Methodology-General Guidance for the Design of Test Rooms*; International Organization for Standardization, Geneva, Switzerland, 1988.

(22) Olsen, E.; Vogt, G.; Saarem, K.; Greibrokk, T.; Nilson, A. Autooxidation of cod liver oil with tocopherol and ascorbyl palmitate. *J. Am. Oil Chem. Soc.* **2005**, *82*, 97–103.

(23) Tauler, R. Multivariate curve resolution applied to second order data. *Chem. Intel. Lab. Sys.* **1995**, *30*, 133–146.

(24) Tauler, R.; Smilde, A.; Kowalski, B. Selectivity, local rank, 3-way data analysis and ambiguity in multivariate curve resolution. *J. Chemometr.* **1995**, *9*, 31–58.

(25) Martens, H.; Naes, T. *Multivariate Calibration*; Wiley: Chichester, U.K., 1989.

(26) Juzenas, P.; Iani, V.; Bagdonas, S.; Rotomskis, R.; Moan, J. Fluorescence spectroscopy of normal mouse skin exposed to 5-aminolaevulinic acid and red light. *J. Photochem. Photobiol. B* **2001**, *61*, 78–86.

(27) Wold, J. P.; Veberg, A.; Nilsen, A.; Iani, V.; Juzenas, P.; Mohan, J. The role of naturally occurring chlorophyll and porphyrins in ligh-induced oxidation of dairy products. A study based on fluorescence spectroscopy and sensory analysis. *Int. Dairy J.* **2005**, *15*, 343–353.

(28) Wold, J. P.; Lundby, F. Approximate non-destructive quantification of porphyrins in butter by front face fluorescence spectroscopy. *J. Animal Feed Sci.* **2007**, *16*, 190–194.

(29) Bekbölet, M. Light effects on food. *J. Food Prot*. **1990**, *53*, 430–440.
(30) Bagdonas, S.; Ma, L. W.; Iani, V.; Rotomskis, R.; Juzenas, P.; Moan, J. Phototransformations of 5-aminolevulinic acid induced protoporphyrin IX in vitro: a spectroscopic study. *Photochem. Photobiol*. **2000**, *72*, 186–192.
(31) Inhoffen, H. H.; Brockmann, H.; Bliesener, K. M. Photoproducts and their transformation into spirographis or isospirographis porphyrin. *Liebigs Ann. Chem*. **1969**, *730*, 173–185.
(32) Cox, G. S.; Bobilier, C.; Whitten, D. G. Photooxidation and singlet oxygen sensitization by protoporphyrin IX and its photooxidation products. *Photochem. Photobiol*. **1982**, *36*, 401–407.
(33) Ericson, M. B.; Grapengiesser, S.; Gudmundson, F.; Wennberg, A. M.; Larkö, O.; Moan, J.; Rosén, A. A spectroscopic study of the photobleaching of protoporphyrin IX in solution. *Lasers Med. Sci*. **2003**, *18*, 56–62.
(34) Veberg, A.; Vogt, G.; Wold, J. P. Fluorescence in aldehydes model systems related to lipid oxidation. *LWT-Food Sci. Technol*. **2006**, *39*, 562–570.
(35) Olsen, E.; Veberg, A.; Vogt, G.; Tomic, O.; Kirkhus, B.; Ekeberg, D.; Nilson, A. Analysis of early lipid oxidation in salmon pâté with cod liver oil and antioxidants. *J. Food Sci*. **2006**, *71*, 284–292.
(36) Yamaki, S.; Kato, T.; Kikugawa, K. Characteristics of fluorescence formed by the reaction of proteins with unsaturated aldehydes. Possible degradation products of lipid radicals. *Chem. Pharm. Bull*. **1992**, *40*, 2138–2142.
(37) Liang., J. H.; Lin, Ch. Ch. Fluorescence kinetics of soybean flour oxidation. *J. Am. Oil Chem. Soc*. **2000**, *77*, 709–713.
(38) Liang, J. H. Fluorescence due to interactions of oxidizing soybean oil and soy proteins. *Food Chem*. **1999**, *66*, 103–108.
(39) Kikugawa, K.; Kato, T.; Beppu, M.; Hayasaka, A. Fluorescent and cross-linked proteins formed by free radical and aldehydes species generated during lipid oxidation. *Lipofuscin and Ceroid Pigments*; Plenum Press: New York, 1990.
(40) Moan, J.; Sommer, S. Oxygen dependence of the photosensitizing effect of hematoporphyrin derivative in NHIK 3025 cells. *Cancer Res*. **1985**, *45*, 1608–1610.
(41) Wessels, J. M.; Sroka, R.; Heil, P.; Seidlitz, H. K. Photodegradation of protoporphyrin-dimethylester in solution and in organized environments. *Int. J. Radiat. Biol*. **1993**, *64*, 475–484.
(42) König, K.; Schneckenburger, H.; Rück, A.; König, R. Studies on porphyrin photoproducts in solution, cells, and tumor tissue. In *Optical Methods for Tumour Treatment and Detection: Mechanisms and Techniques in Photodynamic Therapy III*; Dougherty, T. J., Ed.; SPIE: Bellingham, WA, 1994; Proceedings of SPIE 2133, pp 226−237.
(43) Dietel, W.; Wendenburg, R. The phototransformation of ALA induced protoporphyrin IX (PP IX) in carcinoma cells and of exogenous PPIX in cells and solutions. In *5th International Photodynamic Association Biennial Meeting*; Cortese, D. A., Ed.; SPIE: Bellingham, WA, 1995; Proceedings of SPIE 2371, pp 104-108.
(44) Rotomskiene, J.; Kapociute, R.; Rotomskis, R.; Jonusauskas, G.; Szito, T.; Nizhnik, A. Light-induced transformations of hematoporphyrin diacetate and hematoporphyrin. *J. Photochem. Photobiol. B* **1988**, *2*, 373–379.
(45) Bezdetnaya, L.; Belitchenko, I.; Melnikova, V.; Guillemin, F. Kinetic characteristic of Foscan (MTHPC) and protoporphyrin IX (PP IX) photo-bleaching in solution under oxygen-deficient conditions. In *13th International Congress on Photobiology*; American Society for Photobiology: San Francisco, CA, 2000.
(46) Brown, C. D.; Green, R. L. Critical factors limiting the interpretation of regression vectors in multivariate calibration. *Trends Anal. Chem*. **2009**, *28*, 506–514.

**Received for review January 27, 2010. Revised manuscript received March 12, 2010. Accepted March 15, 2010.**